CONTACT METAMORPHISM IN THE SUPRACRUSTAL ROCKS OF THE SUKUMALAND GREENSTONE BELT IN THE NORTH WEST TANZANIA

N Boniface
University of Dar es Salaam, College of Natural and Applied Sciences, Department of Geology, P. O. Box 35052, Dar es Salaam, Tanzania
Email: nelson.boniface@udsm.ac.tz

ABSTRACT

*Biotite-granite intrusions in meta-ironstones at Geita Hills and the Bukoli alkali-granite intrusion in metabasites at Mawemeru area produced heat that baked the respective country rocks through epidote-amphibolite- to amphibolite-facies. Critical and informative mineral assemblages in the metairostones of Geita Hills are garnet-grunerite-epidote-quartz and garnet-ferrogedrite-biotite-quartz and in the metabasites of Mawemeru is ferrotschermakite-(Na-plagioclase)-quartz. Peak temperatures ranging between 438°C and 544°C were calculated from the above mineral assemblages and a pressure not exceeding 3 kbar was inferred to from the composition of magnesium-iron amphiboles (*grunerite with X_{Fe} ratio of 0.83, i.e. Gru_{83}). *Hornfels textures in the metaironstones are suggested by euhedral poikiloblastic garnet and quartz with grain boundaries intersecting at approximately 120° (granoblastic polygonal texture) and biotite aggregates forming an interlocking network of elongate grains aligned in all directions and bounded by rational crystal faces (decussate texture).*

Keywords. Contact metamorphism, intrusions, Sukumaland Greenstonebelt, Neoarchaean

INTRODUCTION

This paper focuses on contact metamorphic conditions caused by granitic intrusions in supracrustal rocks of the Sukumaland Greenstone Belt at Geita Hills and Mawemeru area. Geita Hills and Mawemeru area form parts of the outer and inner arcs of the Sukumaland Greenstone Belt (Fig. 1).

Stratigraphically the Sukumaland Greenstone Belt belongs to the Neoarchaean Nyanzian Supergroup (Grantham *et al.* 1945). The belt is made up of two intermittently exposed arcs of metavolcanic and metasedimentary rocks surrounded by granitoid rocks (Fig. 1). Barth (1990), Borg (1992), and Borg and Shackleton (1997) reviewed the geological setting and lithostratigraphic subdivisions of the Sukumaland Greenstone Belt. These workers suggested that the inner arc of the Sukumaland Greenstone Belt, which consists of gabbro, pillow basalt and subordinate felsic lava flows and pyroclastics is a representative of the lower Nyanzian Supergroup subdivision. The upper Nyanzian subdivision, which crops out in the outer arc is predominantly composed of banded iron formation (BIF), felsic pyroclastic and lava flows and carbonaceous shales. The upper Nyanzian is overlain unconformably by the Kavirondian coarse clastic metasediments (Barth, 1990). This stratigraphic relationship is consistent with the general stratigraphic arrangement encountered in other greenstone belts of the world (Windley 1995).

A trachyandesite from Geita Hills (Fig. 1), which is interlayered with BIF was dated by Borg and Krogh (1999) at 2699 Ma. Manya and Maboko (2002) interpreted this date to be a minimum age of BIF deposition in the upper Nyanzian subdivision. Episodes of granitic magmatism, which caused contact thermal metamorphism in the Sukumaland Greenstone Belt are dated at 2640-2620 Ma by Bell and Dodson (1981), Maboko *et al.*

(2002). Igneous emplacement of metabasalt of lower Nyanzian occurred at 2823 Ma (Manya and Maboko 2002).

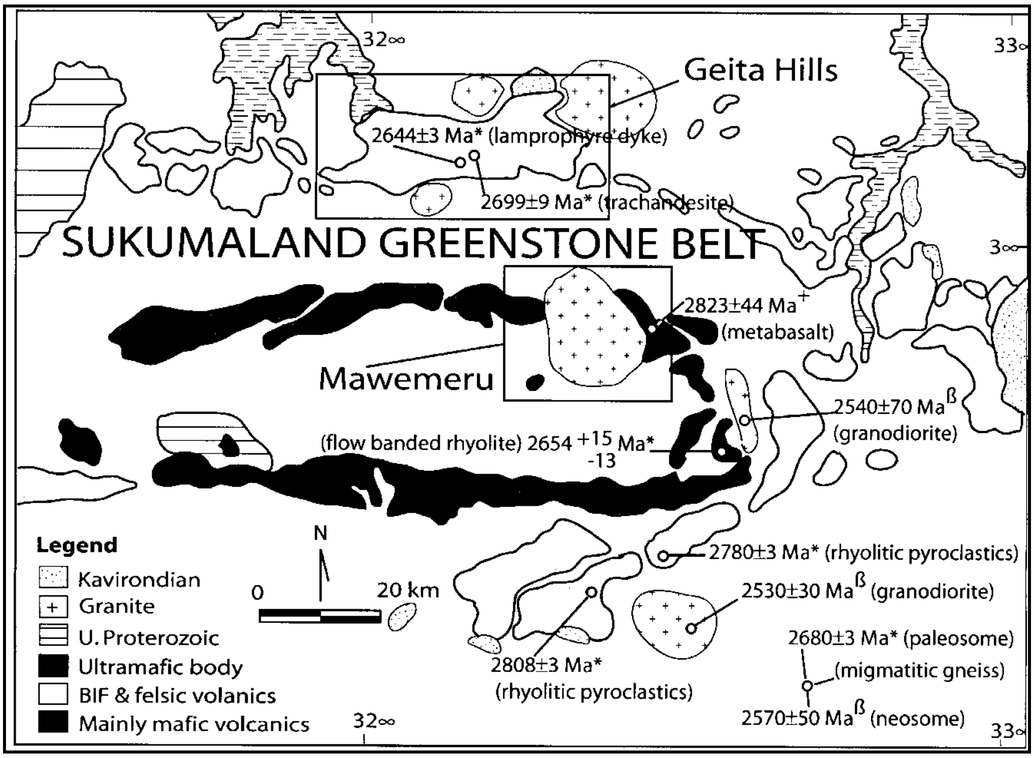

Figure 1: Geological map of the Sukumaland Greenstone Belt showing the location of Mawemeru and Geita Hills (modified from Borg and Shackleton, 1997). Geochronological data; *Borg and Krogh (1999), +Manya and Maboko (2002), § Bell and Dodson (1981).

Low-grade regional metamorphic events (greenshist- to amphibolite-facies) are known to occur in the supracrustal rocks of the Sukumaland Greenstone Belt. In this paper I characterize mineral assemblage and *P-T* conditions in these supracrustal rocks. Granitoids and mafic dykes extensively intrude the supracrustal rocks of the Sukumaland Greenstone Belt and are thought to be sources of heat, which locally caused contact metamorphism in the supracrustal rocks. This work will focus at the effect of Bukoli alkali-post-orogenic granite to the surrounding supracrustal rocks and that of several suites of granodiorites surrounding BIFs at Geita Hills.

MATERIALS AND METHODS

Several supracrustal rock samples of different litho-types were collected from the study areas (Geita Hills and Mawemeru area) along profiles from the granite contact extending into the supracrustal units. Five thin sections were made at the University of Kiel (Germany) from carefully selected rock samples of various rock types. Minerals were analyzed using a 'JEOL Superprobe JXA-8900R' electron microprobe at the University of Kiel. For quantitative analyses the acceleration potential used for analyses was 15 to 20 kV for a beam current of 20 nA. The raw data were corrected by using the CITZAF method (Armstrong, 1995).

RESULTS

Petrography and mineral chemistry

Petrographic data of metaironstone from Geita Hills and metabasites from Mawemeru area show mineral assemblages and mineral compositions of low- to intermediate- grade. Mineral chemical data and constraints of *P-T* conditions of the metaironstones and the metabasites are presented and discussed in turn.

Meta-ironstones

The occurrence of contact metamorphic rocks in at Geita Hills is suggested by the presence of garnet and associated typical hornfels texture in the BIFs. The rocks have layers containing quartz grains with planar grain boundaries intersecting at approximately 120° (granoblastic polygonal texture) and biotite forms interlocking network of elongated grains aligned in all directions forming decussate textures (Fig. 2A&B) typical of hornfels textures found in contact metamorphic rocks heated and equilibrated under static conditions (Winkler 1979). Metamorphic mineral assemblages of the garnet bearing meta-ironstones are garnet-grunerite-epidote-quartz and garnet-ferrogedrite-biotite-quartz. Chlorite occurs as a secondary mineral produced during retrograde reactions.

Garnet

Texturally there are two types of garnets; a euhedral inclusion-poor garnet, and a subhedral to euhedral poikiloblastic garnet rich in randomly oriented amphibole inclusions (Fig. 2C&D). The size of the euhedral inclusion-poor garnet ranges between 110 to 620 mm. Compositionally both types of garnet are similar. Their representative composition is given in Table 1. Garnet is rich in Fe with proportions of almandine reaching up to 86% and X_{Fe} values [X_{Fe}=Fe/(Fe+Mg)] ranging at 0.97-0.98. Their cores are composed of X_{Alm} = 0.82-0.86, X_{Prp} = 0.01-0.02, X_{Grs} = 0.07-0.11, and X_{Sps} = 0.03-0.07. Garnets reveal a slight increase of Ca (X_{Grs}) and a slightly decrease of Mn (X_{Sps}) contents from the core (XGrs=0.07) towards the rims (XGrs=0.11) (Table 1), whereas almandine and pyrope show relatively constant compositions (Fig. 3A). A slight rise in X_{Grs} and drop of X_{Sps} from garnet cores towards garnet rims reflects growth of garnet when pressure was slightly increasing (see Spear 1993).

Biotite

Biotite occurs in aggregates forming interlocking networks among its grains, which are randomly oriented (Fig. 2B). Ti contents in the biotite range between 0.11 and 0.13 and the X_{Fe} varies only in a very limited range from 0.61 to 0.62 (Table 2). In the Ti against X_{Fe} diagram (Fig. 3B) biotite plot in the field of sillimanite-staurolite grade of metamorphism pointing to amphibilite-facies conditions of metamorphism.

Amphiboles

Based on chemical composition amphibole of the meta-ironstones is classified as grunerite and ferrogedrite (Fig. 3C). These amphiboles have very low contents of Na and Ca allowing them to be grouped as magnesium-iron amphiboles on the amphibole classification scheme of Leake *et al.* (1997). Ferrogedrite occurs as coarse elongated laths (230-1070 mm) or as extremely fine fibrous (10-70 mm) in the matrix and as inclusions in garnet (Fig. 2C). Grunerite occurs as an extremely fine, randomly oriented, fibrous mineral in the matrix (Fig. 2D). Grunerite has X_{Mg} [X_{Mg}=Mg/(Fe+Mg)] values ranging between 0.16 and 0.17, and the content of Al in the tetrahedral and octahedral sites is relatively small with maximum values of 0.02 and 0.12 respectively. Content of (Al^{VI}+Fe^{3+}+Ti) in the octahedral site (M2) is relatively low and the content of Na (M4) is extremely small. Ferrogedrite has X_{Mg} values ranging between 0.23 and 0.24. The maximum content of Al in these amphiboles is 1.80 in the tetrahedral site, which is higher than that of the octahedral site at 1.47. The total alkali content in site A is low with maximum value of 0.42 (Table 3).

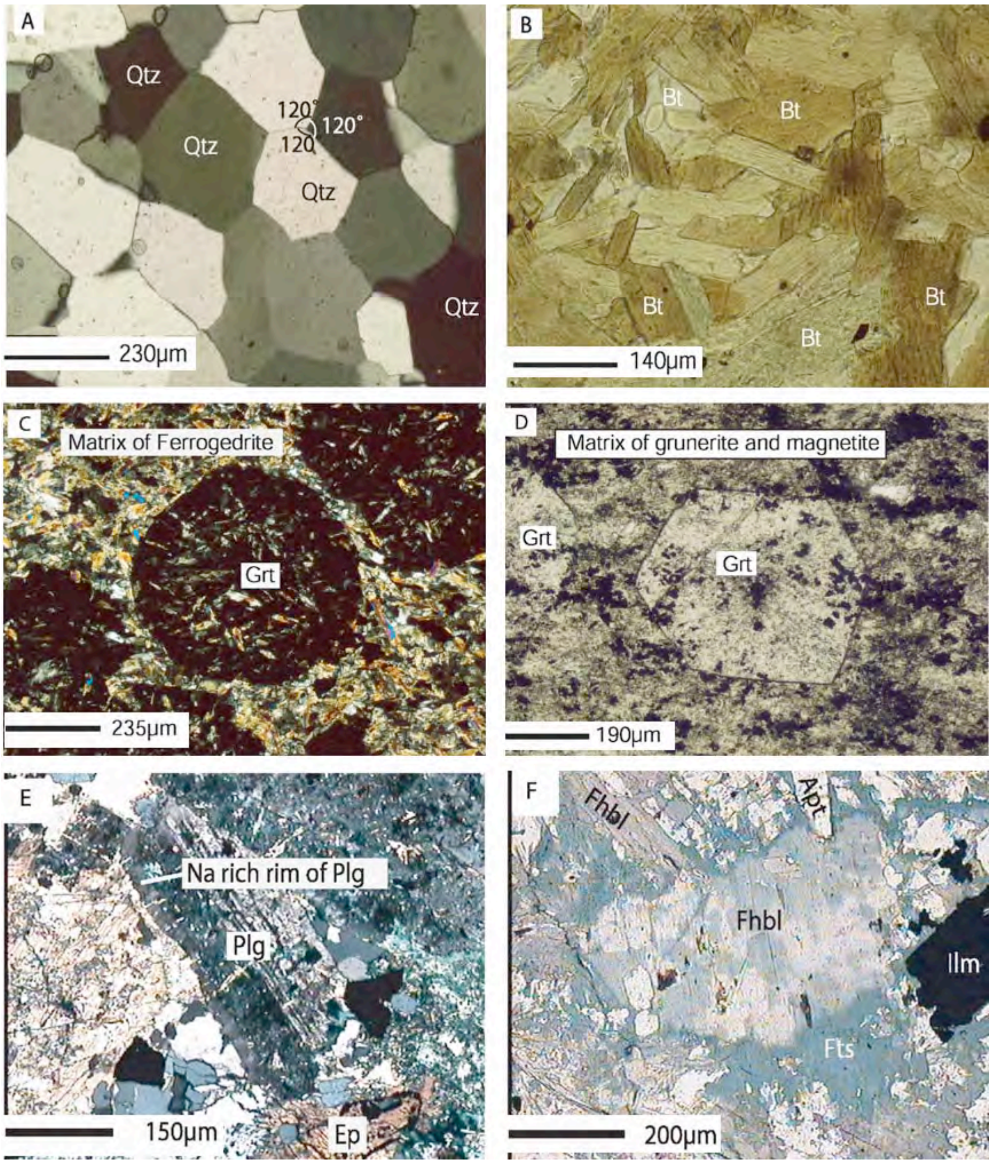

Figure 2: Metamorphic textures in meta-ironstone (A, B, C and D) and metabasite (E and F). (A) granoblastic polygonal textures in quartz (B) Deccusate textures in biotite. (C) Poikiloblastic garnet with randomly oriented ferrogedrite in matrix and as inclusions in garnet. (D) Euhedral garnet in the matrix of grunerite and magnetite. (E) Na-rich metamorphic rim around magmatic plagioclase (F) Metamorphic rim of ferrotschermakite surrounding magmatic core of ferrohornblende.

Table 1: Representative analyses of garnet from meta-ironstone

Sample number N70A													
Garnet													
No.	5	7	8	9	11	13	14	15	16	18	20	21	23
SiO_2	37.16	37.03	37.09	36.87	36.89	36.82	37.12	37.09	37.13	36.78	37.06	36.86	36.97
TiO_2	0.06	0.06	0.12	0.07	0.09	0.01	0.11	0.12	0.16	0.06	0.10	0.11	0.06
Al_2O_3	20.86	20.87	20.70	20.76	20.90	20.76	20.93	20.61	20.61	20.95	20.85	20.75	20.84
FeO	37.01	37.08	37.04	37.47	36.93	37.37	37.25	37.23	37.36	37.46	37.57	37.32	37.22
MnO	1.76	2.05	2.08	2.33	2.65	2.89	3.05	3.10	3.21	2.63	2.38	2.17	1.83
MgO	0.38	0.46	0.46	0.41	0.38	0.37	0.34	0.36	0.40	0.38	0.40	0.43	0.45
CaO	3.93	3.70	3.58	3.06	2.84	2.59	2.61	2.64	2.58	2.74	2.88	2.98	3.84
Total	101.2	101.2	101.1	101.0	100.7	100.8	101.4	101.1	101.5	101.0	101.2	100.6	101.2
Cations: 12 oxygens													
Si	3.003	2.993	3.003	2.995	2.999	2.998	3.001	3.009	3.005	2.988	2.999	3.000	2.991
Ti	0.004	0.004	0.007	0.004	0.005	0.000	0.007	0.007	0.010	0.004	0.006	0.007	0.004
Al	1.986	1.988	1.976	1.988	2.003	1.992	1.994	1.971	1.966	2.005	1.990	1.990	1.987
Fe^{2+}	2.501	2.507	2.508	2.545	2.511	2.545	2.518	2.526	2.529	2.544	2.543	2.540	2.518
Mn	0.121	0.140	0.142	0.160	0.183	0.199	0.209	0.213	0.220	0.181	0.163	0.150	0.125
Mg	0.046	0.056	0.056	0.049	0.046	0.045	0.042	0.043	0.048	0.046	0.048	0.052	0.054
Ca	0.340	0.321	0.311	0.266	0.248	0.226	0.226	0.229	0.224	0.238	0.250	0.260	0.333
Total	8.001	8.008	8.003	8.008	7.995	8.005	7.996	7.998	8.002	8.005	7.999	7.999	8.011
X_{Alm}	0.831	0.829	0.831	0.843	0.840	0.844	0.841	0.839	0.837	0.846	0.846	0.846	0.831
X_{Prp}	0.015	0.018	0.019	0.016	0.015	0.015	0.014	0.014	0.016	0.015	0.016	0.017	0.018
X_{Grs}	0.113	0.106	0.103	0.088	0.083	0.075	0.075	0.076	0.074	0.079	0.083	0.087	0.110
X_{Sps}	0.040	0.046	0.047	0.053	0.061	0.066	0.070	0.071	0.073	0.060	0.054	0.050	0.041
X_{Fe}	0.982	0.978	0.978	0.981	0.982	0.983	0.984	0.983	0.981	0.982	0.981	0.980	0.979

Metabasites

Primary igneous minerals in the gabbroic metabasite of Mawemeru have well-preserved cores, but also have well-developed metamorphic rims or coronas. The primary igneous minerals are ferrohornblende, plagioclase, apatite, ilmenite and quartz. Metamorphic ferrotschermakite form rims around ferrohornblende and Na-plagioclase partly replaces plagioclase (Fig. 2 E&F). The metamorphic mineral assemblage in these roks is ferrotschermakite-Na-plagioclase-quartz.

Amphiboles

Hornblende occurs as randomly oriented, coarse-grained laths with obvious light-green magmatic cores surrounded by metamorphic dark-green rims (Fig. 2F). The needle-like hornblende crystals in the matrix are dark-green similar to the rims of the coarse hornblende and have grown without preferred orientations. Light-green cores of the coarse laths have different chemical composition compared to its dark-green rims. The Ca content in the rim and in the core is high ($Ca_B > 1.5$) placing them in the Ca-amphibole group in the classification scheme of Leake et al. (1997) (Fig. 3D). The light-green cores of amphibole plot in the field of ferrohornblende whereas its dark-green rim plots in the field of ferrotschermakite. Needle-like amphibole grains in the matrix have the chemical composition of ferrotschermakite similar to rims of the coarse laths. M4 site in these amphiboles has intermediate values of Na ranging between 0.01 and 0.45 and the total (Al^{VI}+Fe^{3+}+Ti+Cr) also have intermediate values (Table 3). High values of Na content in site (M4) of amphiboles reflect high metamorphic pressure, which a rock experienced. Al^{IV} content is a measure of edenite exchange and tschermak exchange in amphiboles and other minerals. At low pressure Al is favored in the tetrahedral site (i.e., Al^{IV}) and at higher pressure is favored in the octahedral site (i.e., Al^{VI}) (Laird and Albee 1981).

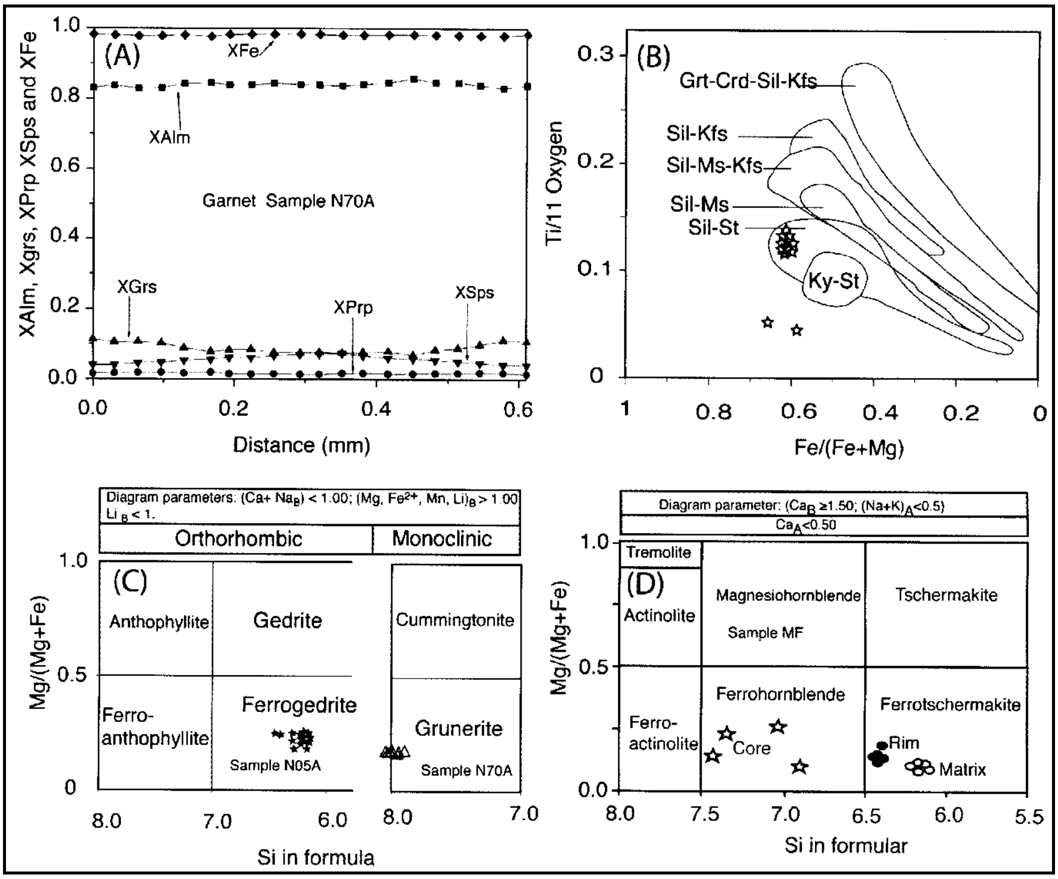

Figure 3: (A) Zoning profile in garnet from meta-ironstone. (B) Plot of Ti (per 11 oxygen) as a function of Fe/(Fe+Mg) for biotites. Note: biotite plot in the field of medium grade, (After Robinson et al. 1982). (C &D) Classification of amphiboles (Leake *et al.* 1997); Amphiboles in meta-ironstones plot in the fields of ferrogedrite and grunerite (Fe-Mg amphiboles) and amphiboles from metabasites plot in the fields of Ferrohornblende and ferrotschermakite (Calcic amphiboles).

Table 2: Representative analyses of biotite and plagioclase

Metaironstone							Metabasite				
Sample N05A: Biotite							Sample MF: Plagioclase				
								core	core	rim	rim
No.	84	85	86	87	88	90	No.	33	34	36	37
SiO_2	34.71	34.81	35.47	34.98	35.66	35.06	SiO_2	60.02	60.21	64.08	64.52
TiO_2	0.97	0.99	1.03	1.06	1.09	1.09	TiO_2	0.00	0.00	0.00	0.00
Al_2O_3	16.25	16.70	16.44	16.01	16.36	16.40	Al_2O_3	25.39	25.21	22.92	22.55
Cr_2O_3	0.08	0.02	0.05	0.05	0.04	0.02	Fe_2O_3	0.22	0.29	0.10	0.03
FeO	24.35	25.26	24.68	24.01	24.02	24.83	CaO	6.87	6.57	3.75	3.94
MgO	8.46	8.47	8.56	8.62	8.76	8.67	Na_2O	7.43	7.91	9.37	8.74
Na_2O	0.21	0.19	0.21	0.21	0.22	0.21	K_2O	0.02	0.06	0.02	0.02
K_2O	8.78	8.84	9.27	8.90	8.54	8.92	Total	99.95	100.25	100.24	99.80
Total	93.92	95.30	95.73	93.91	94.71	95.23					
Cations: 22 oxygen							Cations: 8 oxygen				
Si	5.51	5.46	5.53	5.55	5.57	5.49	Si	2.67	2.68	2.82	2.84
Al^{iv}	2.49	2.54	2.47	2.46	2.43	2.51	Ti	0.00	0.00	0.00	0.00
Al^{vi}	3.02	2.92	3.06	3.09	3.15	2.99	Al	1.33	1.32	1.19	1.17
Ti	0.12	0.12	0.12	0.13	0.13	0.13	Fe^{3+}	0.01	0.01	0.00	0.00
Cr	0.01	0.00	0.01	0.01	0.00	0.00	Ca	0.33	0.31	0.18	0.19
Fe	3.23	3.31	3.22	3.18	3.14	3.26	Na	0.64	0.68	0.80	0.75
Mg	2.00	1.98	1.99	2.04	2.04	2.03	K	0.00	0.00	0.00	0.00
Na	0.06	0.06	0.06	0.06	0.07	0.06	Total	4.98	5.01	4.99	4.95
K	1.78	1.77	1.84	1.80	1.70	1.78					
Total	15.77	15.79	15.79	15.76	15.68	15.79	X_{Ab}	66.06	68.29	81.76	79.93
							X_{An}	33.80	31.39	18.11	19.93
X_{Fe}	0.62	0.63	0.62	0.61	0.61	0.62	X_{Or}	0.13	0.32	0.13	0.14

Table 3: Representative analyses of amphiboles from meta-ironstones and metabasites

Metabasite							Metaironstone					
Sample No. MF	Rim		Core		Matrix needles		Sample No. N70A			Sample No. N05A		
Analysis No.	28	29	30	31	38	39	28	30	32	96	98	100
SiO_2	40.86	40.43	47.72	45.67	38.82	45.51	49.54	49.88	49.69	40.59	40.49	40.34
TiO_2	0.09	0.36	0.58	0.53	0.05	0.12	0.00	0.00	0.00	0.14	0.00	0.07
Al_2O_3	11.42	11.36	1.75	4.49	14.03	13.78	0.65	0.76	0.49	18.14	17.66	17.73
Cr_2O_3	0.00	0.00	0.00	0.00	0.00	0.00	0.00	0.00	0.00	0.12	0.10	0.05
Fe_2O_3	6.94	7.56	0.01	19.04	7.59	0.00	0.00	0.00	0.00	0.00	0.00	0.00
FeO	23.20	23.00	37.76	16.33	22.67	24.85	41.23	41.57	41.59	31.74	32.02	32.40
MnO	0.27	0.27	0.88	0.53	0.31	0.27	0.28	0.28	0.19	0.10	0.09	0.17

MgO	2.1(	1.89	3.6(	3.21	1.52	1.5:	4.7(	4.92	4.7:	5.4(	5.66	5.3:
CaO	10.71	10.35	4.4:	7.96	10.80	9.5<	0.3:	0.24	0.3(	0.3(	0.37	0.4:
Na_2O	1.31	1.53	0.2<	0.55	1.61	2.7(	0.0(	0.09	0.0(	1.8:	1.88	1.9(
K_2O	0.5<	0.49	0.1:	0.19	0.65	0.4:	0.01	0.01	0.01	0.0(	0.00	0.0(
H_2O*	1.9(	1.89	1.8(	1.95	1.90	1.9(	1.8(	1.87	1.8(	1.9(	1.95	1.9:
Total	99.:	99.1	99.1	100.5	100.0	100.(	98.:	99.6	99.1	100.<	100.2	100.<
Cations: 23 oxygen												
Si	6.4:	6.40	7.71	7.02	6.11	6.8(	8.0(	7.98	8.0(	6.2(	6.22	6.2(
Al iv	1.5:	1.60	0.2(	0.81	1.89	1.1:	0.0(	0.02	0.0(	1.8(	1.78	1.8(
Al vi	0.5:	0.52	0.0<	0.00	0.71	1.3<	0.1:	0.12	0.0(	1.4:	1.41	1.41
Ti	0.01	0.04	0.0:	0.06	0.01	0.01	0.0(	0.00	0.0(	0.0:	0.00	0.01
Cr	0.0(	0.00	0.0(	0.00	0.00	0.0(	0.0(	0.00	0.0(	0.01	0.01	0.01
Fe^{3+}	0.8:	0.90	0.0(	2.20	0.90	0.0(	0.0(	0.00	0.0(	0.0(	0.00	0.0(
Fe^{2+}	3.0(	3.05	5.1(	2.10	2.98	3.1<	5.5:	5.56	5.6(	4.0(	4.11	4.1(
Mn	0.0<	0.04	0.1:	0.07	0.04	0.0:	0.0<	0.04	0.0:	0.01	0.01	0.0:
Mg	0.4(	0.45	0.8(	0.74	0.36	0.3:	1.1:	1.17	1.1:	1.2:	1.30	1.2:
Ca	1.81	1.76	0.7:	1.31	1.82	1.5:	0.0:	0.04	0.0:	0.0:	0.06	0.0(
Na	0.4(	0.47	0.0:	0.16	0.49	0.8:	0.0:	0.03	0.0:	0.5<	0.56	0.5:
K	0.11	0.10	0.0:	0.04	0.13	0.0(	0.0(	0.00	0.0(	0.0(	0.00	0.0(
OH*	2.0(	2.00	2.0(	2.00	2.00	2.0(	2.0(	2.00	2.0(	2.0(	2.00	2.0(
Total	17.3:	17.33	17.1(	16.51	17.44	17.3:	16.9:	16.96	16.9(	17.41	17.46	17.4:
(Ca+Na) (B)	2.0(	2.00	0.7(	1.48	2.00	2.0(	0.0<	0.04	0.0(	0.2:	0.21	0.2:
Na (B)	0.1(	0.24	0.1(	0.28	0.18	0.4:	0.0:	0.03	0.0:	0.1:	0.15	0.1<
(Na+K) (A)	0.3:	0.33	0.0<	0.21	0.44	0.4<	0.0(	0.00	0.0(	0.3:	0.41	0.4:
Fe/(Fe+Mg)	0.8(	0.87	0.8:	0.74	0.89	0.9(	0.8:	0.83	0.8:	0.2<	0.24	0.2:

Plagioclase

Plagioclase laths also have well-developed metamorphic rims around well-preserved magmatic cores (Fig. 2E). The plagioclase cores are Ca richer with X_{An}=0.31-0.34 (andesine) than the surrounding rims with X_{An}=0.18-0.20 (oligoclase) indicating a re-equilibration of magmatic plagioclase at lower metamorphic temperatures than magmatic temperatures at which Ca-rich plagioclase formed. Oligoclase composition in plagioclase rims reflects it recrystallization in the amphibolite-facies conditions (Turner and Verhoogen 1960).

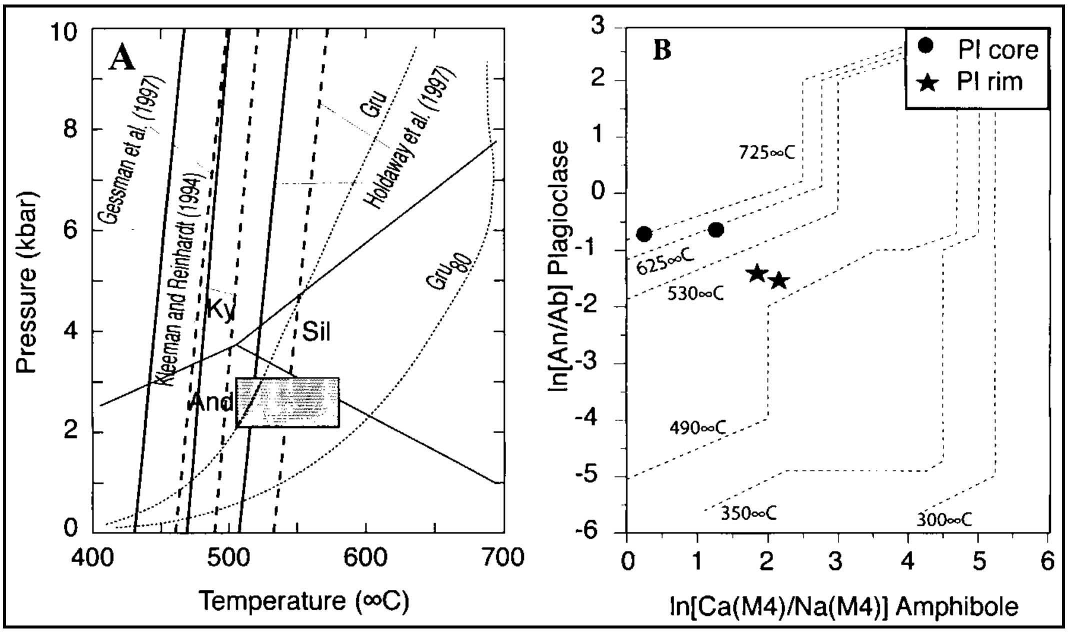

Figure4: Geotherometers (A) P-T diagram showing the results of garnet-biotite geothermometry using various calibrations. The solid and dashed curves represent rims and cores of garnet, respectively. The box highlight the stability field of grunerite bearing mineral assemblage in iron formations of Negaunee (Haase 1982) which lies between Grunerite with XFe=80 (Gru80) and that with XFe=100 (Gru100). (B) Graphical geothermometer of Spear (1980) which uses the Ca and Na exchange equilibrium between amphibole and plagioclase from a metabasite sample.

Geothermobarometry

Meta-ironstone

The equilibrium mineral assemblage garnet-biotite-chlorite in meta-ironstones of the Geita Hills allows the use of Fe-Mg exchange geothermometers between garnet-biotite, and garnet chlorite, to estimate temperatures at which these minerals formed. Unfortunately this assemblage is not useful for pressure calculations. Several Fe-Mg exchange between garnet-biotite geothermometers were used for temperature estimations; they include calibrations of Ferry and Spear (1978), Perchuk and Lavrent'eva (1981), Hodges and Spear (1982), Ganguly and Saxena (1984), Indares and Martignole (1985), Kleemann and Reinhardt (1994), Gessmann et al. (1997) and Holdaway *et al.* (1997). These broad number of geothermometers give a relatively narrow and reasonable range of temperature values at 438-544°C in the stability field of Gru80 at a pressure of 2-3 kbar (Fig. 4A). The values of pressure between 2 kbar and 3 kbar are assumed by considering the stability fields of grunerite (Gru80) at low temperatures (Haase 1982) (Fig. 4A). The X_{Fe} ratio for grunerite in the meta-ironstone sample number N70A is 0.83 (Table 3) so it is reasonable to assume a maximum pressure condition of 3 kbar during contact metamorphic imprints in meta-ironstones.

These results can be compared with information obtained from experimentally determined stability fields of Fe-Mg amphiboles. Evans and Lattard (1992), in experiments on the stability of grunerite, concluded that grunerite has a maximum thermal stability of 650±20°C at 9.7±1kbar at an invariant point on the reaction curve. Similar stability fields of grunerite-bearing mineral assemblages in several iron formations are known from works of different authors (e.g. Immega and Klein 1976, Klein 1978, Gole and Klein 1981, Haase 1982).

Metabasite

The application of the plagioclase-hornblende graphical geothermometer of Spear (1980), which uses the Ca and Na exchange equilibrium between plagioclase and hornblende, was employed to estimate the temperature of thermal metamorphism in the metabasites of Mawemeru area. Plagioclase cores are rich in Ca and therefore yield higher magmatic temperatures between 625°C and 725°C. The rims have lower Ca contents than the cores reflecting plagioclase recrystallizing at lower temperatures, 500°C, during metamorphism (Fig. 4C).

DISCUSSION AND CONCLUSIONS

The metamorphic mineral assemblages in meta-ironstone, ferrogedrite-garnet (almandine-rich)-biotite-quartz and garnet-grunerite-epidote-quartz, are stable under medium-grade (amphibolite-facies) metamorphic conditions (Winkler 1979, Yardley 1990, Spear 1993). Likewise the metamorphic mineral assemblage for the metabasites, ferrotschermakite-albite-quartz-epidote, belongs to the medium-grade (epidote-amphibolite-facies) metamorphic conditions (Spear 1993). The metamorphic conditions inferred to from these mineral assemblages conform to the range of the calculated temperatures using Fe-Mg exchange geothermometers, which is between 438°C and 544°C for the meta-ironstones, and at 500°C for the metabasites when the plagioclase-amphibole geothermometer of Spear (1980) is used. These temperature ranges conform to the epidote-amphibolite-facies and garnet-amphibolite facies of metamorphism (Yardley 1990, Spear 1993).

The chemical composition of biotite from the meta-ironstones suggests *P-T* conditions of intermediate grade during the metamorphism. The plot of Ti against Fe/(Fe+Mg) falls in the field of sillimanite-staurolite (Robinson *et al*. 1982), which is equivalent to amphibolite-facies conditions. Na in (M4) site of amphiboles is a measure of pressure of metamorphism and also Al^{IV} content is a measure of edenite exchange and tschermak exchange in amphiboles and other minerals. At low pressure Al is favoured in the tetrahedral site (i.e., Al^{IV}) and at higher pressure is favoured in the octahedral site (i.e., Al^{VI}). The contents of Na (M4) and total alkali (Na+K)(A) in amphiboles from the meta-ironstones and from the metabasites suggest that metamorphism in these rocks took place in conditions of low pressures and intermediate temperatures. These mineral composition support medium temperature range 438-544°C calculated from the meta-ironstones and metabasites.

The emplacement of granites in the Neoarchaen supracrustal rocks of the Sukumaland Greenstone Belt caused contact metamorphic aureoles in the neighboring meta-ironstones and metabasites. The peak of this thermal metamorphic imprint in these rocks was up to amphibolite-facies at low pressures not exceeding 3 kbar and medium temperatures of up to 544°C. Biotite-granite intrusions in the meta-ironstones at Geita Hills and the Bukoli alkali-granite intruding the metabasites at Mawemeru produced heat that baked the respective country rocks through epidote-amphibolite- to amphibolite-facies.

ACKNOWLEDGEMENTS

Sida/SAREC funded the fieldwork under the program Research Capacity Development at geology department and DAAD sponsored a short visit to Germany. I wish to express my sincere gratitude to Prof. Abdul Mruma for his constructive inputs and support, Prof. Dr. Volker Schenk for allowing all the analyses and petrographic studies to be conducted in the laboratories at the

University of Kiel and Dr. Peter Appel for mineral chemistry analyses, Mr. John Hill of Geita Gold Mine for his logistical support in the field at Geita Gold Mine.

REFERENCES

Armstrong JT 1995 CITZAF a package of correction programs for the quantitative electron microbeam X-ray analysis of thick polished materials, thin films and particles. *Microbeam Analysis*, 4, 117–200.

Barth H 1990 Provisional Geological map of Lake Victoria gold field, Tanzania.Hannover, 59p. Bearth, P. 1962: Schweiz. *Mineral. Petrog. Mitt.* **43**: 127-137.

Bell K and Dodson MH 1981 The geochronology of the Tanzania shield. *J. Geol.* **89**: 109-229.

Borg G 1992 New aspects on the lithostratigraphy and evolution of Siga hills, an Archaean granite-Greenstone terrain in NW-Tanzania. Zeitschrift Angrewandte Geologie. **38**: 89-93.

Borg G and Krogh T 1999 Isotopic age data of single zircon from the Archaean Sukumaland Greenstone Belt. Tanzania. *J. Afr. Earth Sci.* **29**: 301-312.

Borg G and Shackleton RM 1997 The Tanzania and NE Zaire Craton. In: de Wit, M.J. Ashwal, L.D. (Eds.) Greenstone belts. Clarendon Press Oxford, 608-619.

Evans BW and Lattard D 1992 New experiments on the stability of grunerite. *Eur. J. Mineral*. 4, 219-238.

Ferry JM and Spear FS 1978 Experimental calibration of the partitioning of the Fe and Mg between biotite and garnet. *Contribution to the mineralogy and petrology*, **71**: 13-22.

Ganguly J and Saxena SK 1984 Mixing properties of aluminosilicate garnets: Constraints from natural and experimental data, and applications to geothermobarometry: *Am. Mineral.* **69**: 88-97.

Gessmann CK, Spiering B and Raith M 1997 Experimental study of the Fe-Mg exchange between garnet and biotite: Constraints on the mixing behavior and analysis of the cation exchange mechanisms: Am. *Mineral.* **82**, 1225-1240.

Gole MJ and Klein C 1981 High-grade metamorphic Archaean banded iron formations, Western Australia: Assemblages with coexisting paroxenes ±fayalite. *Am. Mineral*, **66**: 87-99.

Grantham DR, Temperley BN and McConnell RB 1945 Explanation of the Geology of the degree sheet No. 17 (Kahama). Geological Survey of Tanganyika Bulletin. **15**, 1-32, Dar es Salaam.

Haase CS 1982 Metamorphic petrology of the Negaunee iron formation, Marquette district, northern Michigan: Mineralogy, metamorphic reactions and phase equilibria. *Economic Geology,* **77**: 60-81.

Hodges KV and Spear FS 1982 Geothermometry and the Al_2SiO_5 triple point at Mt. Mooslauke, New Hampshire. *Am. Mineral.* **67**: 1118-1134

Holdaway MJ, Mukhopadhyay B, Dyar MD, Guidotti CV and Dutrow BL 1997 Garnet-biotite geothermometry revised: new Margules parameters and a natural specimen data set from Maine. *Am. Mineral.* **82**: 582-595.

Immega IP and Klein C 1976 Mineralogy and petrology of some metamorphic Precambrian iron formations in Southwestern Montana. *Am. Mineral.* **61**: 1117-1144.

Indares A and Martignole J 1985 Biotite –garnet geothermometry in the granulite facies: the influence of Ti and Al in Biotite. *Am. Mineral.* **70**: 272-278.

Kleemann U and Reinhardt J 1994 Garnet-Biotite thermometry revised: the effect of Al^{VI} and Ti in Biotite. *Eur. J. Mineral*. **6**: 625-941.

Klein C 1978 Regional metamorphism of Proterozoic iron formation, Labrador Trough, Canada. *Am. Mineral.* **63**: 898-912.

Laird J and Albee AL 1981 Pressure-temperature and time indicators in mafic schist: their application to reconstructing the polymetamorphic history of Vermont. *Am. J. Sci*. **281**: 127-175

Leake BE, Woolley AR, Arps CES, Birch WD, Gilbert MC, Grice JD, Hawthorne FC, Kato A, Kisch HJ, Krivovichev VG, Lintjout K, Laird J, Mandarino J, Maresch WV, Nickle EH, Rock NMS, Schumacher JC, Smith DC, Stephenson NCN, Ungaretti L, Whittaker EJW and Youzhi G 1997 Nomenclature of amphiboles. Report of the Subcommittee on Amphiboles of the International Mineralogical Association Commission on New Minerals and Mineral Names. *Eur. J. Mineral.* **9**: 623-651.

Maboko MAH, Manya S, Torssander P and Pedersen RB, 2002 Isotopic and geochemical investigation of the granitoids in the Sukumaland Greenstone belt of the Northern Tanzania. Constraints on Archaean crustal growth in the Tanzania Craton. *Precambrian Research*.

Manya S, and Maboko MAH, 2002 Dating basaltic volcanism in the Neoarchaean Sukumaland Greenstone Belt of the Tanzania Craton using the Sm-Nd method: Implications for the geological evolution of the Tanzania Craton. *Precamb. Res.* **121**, 35-45

Perchuk LL and Lavrant´eva IV, 1981 Experimental investigation of exchange equilibria in the system cordierite-garnet-biotite. In: Saxena, S.K., ed. Kinetics and equilibrium in mineral reactions. Spinger Verlag, 199-240.

Robinson PR, Hollocher KT, Tracy RJ and Dietsche CW 1982 High grade Acadian regional metamorphism in south-central Massachusetts. In: Joesten R, Quarrier S. (eds) NEIGC 74th Ann Mtg. State Geology and Natural History Surv. Connecticut, Storrs, CT, 289-340

Spear FS 1980 The gedrite-anthophyllite solvus and the composition limits of the orthoamphibole from the post pond volcanics, Vermont. *Am. Mineral*. **65**: 1103-1118.

Spear FS, 1993 Metamorphic Phase Equilibrium and Pressure-Temperature-Time Paths. Mineralogical Society of America MONOGRAPH, Washington, D.C. 799p

Turner FJ and Verhoogen J 1960 Igneous and metamorphic petrology McGraw-Hill Book company, New York. 694p

Windley BF 1995 The evolving continents 3rd edn. Wiley and, chichester, 526p.

Winkler HGF 1979 Petrogenesis of metamorphic rocks. 5th edn. Springer-Verlag New York Heidelberg Berlin. Germany, 348p.

Yardley BWD, 1990 An introduction to metamorphic petrology, Longman Scientific and Technical, co-publisher, John Wiley & sons, Inc., New York. 248p